Citation: A. Gonzalez, M. Aranda, G. Lopez-Nicolas, C. Sagues. Time delay compensation based on Smith Predictor in multiagent formation control. IFAC 2017 World Congress, International Federation on Automatic Control. pp 11963-11969, Toulouse, July 9-14, 2017.

Time delay compensation based on Smith Predictor in multiagent formation control

Antonio González * **Miguel Aranda** ** **Gonzalo López-Nicolás** *
Carlos Sagüés *

* *Inst. de Investigación en Ingeniería de Aragón - Universidad de Zaragoza, C /María de Luna 1, E-50018 Zaragoza, Spain (e-mail: angonsor@gmail.com,gonlopez@unizar.es,csagues@unizar.es).*
** *SIGMA, Institut Pascal, 4 Avenue Blaise Pascal, 63178 Aubière Cedex, France (e-mail: miguel.aranda@sigma-clermont.fr)*

Abstract: This paper investigates the use of time delay compensation methodology based on Smith Predictor applied to the control of a group of agents moving on a plane to a desired rigid geometric configuration. The unavoidable presence of time delays inherent to the communication links between agents is known to have a negative impact on the system performance, leading to instability in some cases. The decentralized and nonlinear nature of the underlying control problem has been taken into account to find a suitable control scheme that counteracts the effect of time delays. Moreover, the control scheme works using relative position measurements expressed in local frames, not being necessary a global coordinate reference frame. It is theoretically demonstrated and confirmed by simulation that exponential stability to the prescribed formation is achieved when time delays are constant and known. Finally, further simulation results show that, even when there exist errors on time delays knowledge, the global system performance is significantly improved with respect to the case of no delay compensation.

Keywords: Multiagent systems, Formation stabilization, Delay compensation

1. INTRODUCTION

The control of multiagent groups has a great number of applications, such as search and rescue missions, autonomous multivehicle control, cooperative sensing, etc. This paper is focused on the specific case of controlling the agents to a desired geometric configuration (Mesbahi and Egerstedt (2010); Oh et al. (2015)). Different approaches have been proposed in this vein, (Ren and Atkins (2007); Zavlanos and Pappas (2007); Sabattini et al. (2011)). In particular, it is of practical interest to consider that only relative position measurements between agents are available (Dimarogonas and Kyriakopoulos (2008); Coogan and Arcak (2012); Oh and Ahn (2014)), and taking one step further it can be assumed that the agents' measurement frames are not equally oriented (Krick et al. (2009); Tian and Wang (2013); Aranda et al. (2015)). In this latter case, no global reference has to be shared by the agents, which increases the flexibility, simplicity and autonomy. For instance, they can operate in a GPS-denied environment by using the locally referred information coming from their independent onboard sensors.

With this motivation, we consider the control framework of Aranda et al. (2015) as a starting point here. A relevant issue for this controller is the presence of time delays, which appear due to multi-hop communication between agents. Indeed, due to time delays, the control action is actually computed by each agent using *past* information regarding the position vectors of its neighbors. This is expected to have a negative impact on the overall system performance, leading even to instability when such delays are large enough, as studied in Aranda et al. (2015). Therefore, it is key to consider time delays in the design and stability analysis of such system (Gu et al. (2003)). In our case, the problem becomes even more complex because the system model is nonlinear and, in addition, interconnected (Papachristodoulou et al. (2010); Nedić and Ozdaglar (2010)).

On the other hand, time delay compensation techniques (or dead-time compensator (DTC) schemes) are widely implemented in processes with constant input/output delay to improve the closed-loop performance of classical controllers (Normey-Rico (2007)). The underlying idea of such approaches is to eliminate the delay from the characteristic equation. In particular, the Smith Predictor (S.P.) (Smith (1957)) and their modifications (Hang et al. (2003); Roca et al. (2014)) have been widely used in many applications involving time delays (see Garrido et al. (2016); Khajorntraidet et al. (2015) and references therein).

Motivated by the practical interest of facing up with time delays in the formation controller, our novel contribution in this paper is to define a delay compensation scheme based on the Smith Predictor. The design of the control scheme will be suitably addressed, taking into account the decentralized and nonlinear nature of the underlying control problem. The predictor uses the knowledge of the values of the time delays in the system. When there are no time delays, the original controller (Aranda et al. (2015)) makes the agents converge exponentially to the desired formation. It is shown that the approach proposed here preserves this property in the presence of time delays, regardless of their values. It is worthwile to

⋆ This work was supported by French Government research program Investissements davenir through the RobotEx Equipment of Excellence (ANR-10-EQPX-44) and the LabEx IMobS3 (ANR7107LABX716701), and by Spanish Government/European Union through project DPI2015-69376-R.

mention the following advantages associated with the proposed scheme:

- The S.P. does not require to add new onboard sensors. Indeed, the S.P. uses the same available information as the control scheme without S.P., that is, the relative position measurements (subject to time delays) and their time-stamps. The latter allows to measure the time delays that will be implemented on the S.P.
- The S.P. is compatible with the use of relative position measurements expressed in local frames, not being necessary to have a global reference frame.
- Even if the overall system is stable (i.e., the desired formation is achieved), the delays can affect the paths followed by the agents significantly. Then, the proposed use of S.P. contributes to restore the efficient trajectories that the controller produces when there are no delays. This efficiency is important as, e.g., it can help to predict interagent collisions, and it decreases the distances travelled by the agents, reducing energy consumption.
- Even if the values of delays used by the predictor scheme are affected by errors, the performance of the system improves significantly in comparison with the case where no delay compensation is implemented.

The paper is organized as follows: Section 2 describes the problem statement, Section 3 describes the proposed delay compensation scheme and implementation details, Section 4 gives a theoretical proof of the stability of the system, followed by simulation results in Section 5, which illustrate the achieved improvement by comparing with the state-feedback control without delay compensation. Finally, conclusions and perspectives are gathered in Section 6.

2. PROBLEM STATEMENT

Consider a set $\mathcal{N}$ of N agents in $\mathcal{R}^2$. The dynamics of the position vector $q_i \in \mathcal{R}^2$ of each agent $1 \leq i \leq N$ is modelled using a single integrator: $\dot{q}_i(t) = u_i(t)$, where $u_i(t) \in \mathcal{R}^2$ is the control input. A prescribed spatial configuration is defined through a reference layout of the agents in their configuration space. We denote as $c_{ki} \in \mathcal{R}^2$ the vector from k to i in this reference layout. Thus, these interagent relative position vectors c_{ki} encode the desired configuration. Also, we define the relative position between agent k and i as $q_{ki}(t) = q_k(t) - q_i(t)$. It is assumed that the agents are not interchangeable: each of them has a fixed place in the target formation.

The formation controller in Aranda et al. (2015) makes the agent positions reach the desired configuration, up to a global arbitrary rotation and translation. Each agent uses a control law that follows the negative gradient of a cost function which is computed from the relative positions of the other agents. The cost function encapsulates the formation objective, and includes a rotation matrix defined in such a way that the control law can be computed in each agent's local coordinate frame.

The agents are considered to form a nearest-neighbor communication network so that they obtain the relative position information coming from the rest of agents via multi-hop propagation, which is inherently affected by time delays. We define the delay from agent k to agent i as τ_{ki} and $\bar{\tau} = max(\tau_{ki})$.

The following assumptions are made in this paper:

Assumption 1. The agents have synchronized clocks, a common practical requirement in networked multiagent systems (Schwager et al. (2011)). Also, all the agents start moving at the same instant $\bar{\tau} = max(\tau_{ki})$, i.e., when all the relative position measurements are available for each agent.

Assumption 2. The time delay τ_{ki} is assumed to be time-constant and not necessarily symmetric: $\tau_{ki} \neq \tau_{ik}$. We also consider that every relative position measurement has an associated time stamp, allowing for agent i to measure the τ_{ki} associated to the relative position measurement $q_{ki}(t - \tau_{ki})$.

Assumption 3. Each agent i obtains the measurements of the relative positions of all the rest of agents $k \in \mathcal{N}_i$ with respect to its local reference frame [1].

The formation control problem is posed as the minimization of the following cost function:

$$J_i(t) = \frac{1}{4} \sum_{k \in \mathcal{N}_i} \sum_{j \in \mathcal{N}_i} ||q_{kj}(t) - R(\alpha_i(t)) c_{kj}||^2. \tag{1}$$

The set $\mathcal{N}_i$ includes the neighboring agents of i in the formation graph and agent i as well. We consider in this paper that $\mathcal{N}_i = \mathcal{N}$, $\forall i$. The rotation matrix of the reference layout is defined as:

$$R(\alpha_i(t)) = \begin{bmatrix} cos(\alpha_i(t)) & -sin(\alpha_i(t)) \\ sin(\alpha_i(t)) & cos(\alpha_i(t)) \end{bmatrix} \tag{2}$$

The rotation angle $\alpha_i(t)$ that minimizes $J_i(t)$ at each instant is obtained from the condition $\frac{\partial J_i}{\partial \alpha_i} = 0$, which renders:

$$\alpha_i(t) = atan2 \left(\frac{\sum_{k \in \mathcal{N}_i} \sum_{j \in \mathcal{N}_i} q_{kj}^T(t) c_{kj}^{\perp}}{\sum_{k \in \mathcal{N}_i} \sum_{j \in \mathcal{N}_i} q_{kj}^T(t) c_{kj}} \right), \tag{3}$$

where $c_{kj}^{\perp} = \left((0,1)^T, (-1,0)^T\right) c_{kj}$. Possible degenerate cases for this expression can be disregarded (Aranda et al. (2015)). From Assumption 3, each agent obtains a set of delayed measurements $q_{ki}(t - \tau_{ki})$, $k \in \mathcal{N}_i$ corresponding to the relative positions with respect to itself. The control law is obtained as the negative gradient of the cost function $J_i(t)$ in (1) with respect to $q_i(t)$:

$$u_i(t) = K \sum_{k \in \mathcal{N}_i} e_{ki}(t) \tag{4}$$

$$e_{ki}(t) = q_{ki}(t - \tau_{ki}) - R(\tilde{\alpha}_i(t)) c_{ki}$$

where $K > 0$ is a control gain, and the rotation angle is therefore computed using the available delayed measurements as:

$$\tilde{\alpha}_i(t) = atan2 \left(\frac{\sum_{k \in \mathcal{N}_i} \sum_{j \in \mathcal{N}_i} \tilde{q}_{kj}^T(t) c_{kj}^{\perp}}{\sum_{k \in \mathcal{N}_i} \sum_{j \in \mathcal{N}_i} \tilde{q}_{kj}^T(t) c_{kj}} \right) \tag{5}$$

where $\tilde{q}_{kj}(t) = q_{ki}(t - \tau_{ki}) - q_{ji}(t - \tau_{ji})$. In Aranda et al. (2015), it was studied that large time delays compromise the convergence to the desired formation with this controller. Thus, our goal here is to compensate the effects of the delays, by using the scheme described in the next section.

3. SMITH PREDICTOR-BASED FORMATION CONTROL

The basic idea of the S.P. applied to this problem is to obtain a prediction of the relative position $q_{ki}(t)$ (namely $\hat{q}_{ki}(t)$), computed from the available delayed measurements. Then, the prediction $\hat{q}_{ki}(t)$ will be used in the control law instead of the delayed measurements $q_{ki}(t - \tau_{ki})$. Define the new control law:

$$u_i(t) = \begin{cases} K \sum_{k \in \mathcal{N}_i} \varepsilon_{ki}(t) & t \geq \bar{\tau} \\ 0 & t < \bar{\tau} \end{cases} \tag{6}$$

[1] In the sequel, for the sake of simplicity of the notation, all the vector positions are expressed by default in an arbitrary global reference frame.

where the parameter $\varepsilon_{ki}(t)$ is the error between the rotated spatial reference $R(\hat{\alpha}_i(t))c_{ki}$ and the prediction of the relative position, defined later in (12):

$$\varepsilon_{ki}(t) = \hat{q}_{ki}(t) - R(\hat{\alpha}_i(t))c_{ki} \tag{7}$$

The rotation matrix of the reference layout computed by each agent is defined as:

$$R(\hat{\alpha}_i(t)) = \begin{bmatrix} cos(\hat{\alpha}_i(t)) & -sin(\hat{\alpha}_i(t)) \\ sin(\hat{\alpha}_i(t)) & cos(\hat{\alpha}_i(t)) \end{bmatrix} \tag{8}$$

The rotation angle is therefore obtained from the available predictions $\hat{q}_{ki}$, $k \in \mathcal{N}_i$ as:

$$\hat{\alpha}_i(t) = atan2\left(\frac{\sum_{k\in\mathcal{N}_i}\sum_{j\in\mathcal{N}_i}\hat{q}_{kj}^T(t)c_{kj}^{\perp}}{\sum_{k\in\mathcal{N}_i}\sum_{j\in\mathcal{N}_i}\hat{q}_{kj}^T(t)c_{kj}}\right) \tag{9}$$
$$\hat{q}_{kj} = \hat{q}_{ki}(t) - \hat{q}_{ji}(t)$$

Note that $\hat{\alpha}_i(t)$ minimizes the cost function:

$$\hat{J}_i(t) = \frac{1}{4}\sum_{k\in\mathcal{N}_i}\sum_{j\in\mathcal{N}_i}||\hat{q}_{kj}(t) - R(\hat{\alpha}_i(t))c_{kj}||^2 \tag{10}$$

On the other hand, the delay compensation control scheme is detailed in Fig. 1 and 2. The proposed structure, justified later in Section 4, involves multiple Smith Predictor (S.P) subsystems that allow to obtain the prediction of all the relative positions of the neighboring agents. The internal state $z_{ki}(t)$ of each S.P subsystem is defined as follows:

$$\dot{z}_{ki}(t) = \begin{cases} u_{ki}(t) & t \geq \bar{\tau} \\ 0 & t < \bar{\tau} \end{cases} \tag{11}$$

where $u_{ki}(t) = -KN\varepsilon_{ki}(t)$ and $\varepsilon_{ki}(t)$ is defined in (7). The initial condition for $z_{ki}(t)$ can be taken $z_{ki}(0) = 0$ without loss of generality. Finally, the prediction $\hat{q}_{ki}(t)$ is obtained from $z_{ki}(t)$ and the delayed measurements $q_{ki}(t-\tau_{ki})$ as follows:

$$\hat{q}_{ki}(t) = z_{ki}(t) - z_{ki}(t-\hat{\tau}_{ki}) + q_{ki}(t-\tau_{ki}) \tag{12}$$

where $\hat{\tau}_{ki}$ are the values of time delays to be implemented in the Smith Predictor.

Also, note that $t - \tau_{ki} \geq 0$ since all the agents start their motion in $t = \bar{\tau} = max(\tau_{ki})$ (see Assumption 2). Therefore, both the delayed data $z_{ki}(t-\tau_{ki})$ and $q_{ki}(t-\tau_{ki})$ are available in (12).

4. STABILITY ANALYSIS

This section proves that, when the delays are constant and known ($\hat{\tau}_{ki} = \tau_{ki}$), the proposed delay compensation scheme guarantees the exponential stability of the overall system to the prescribed formation, regardless the value of delays. Prior to the main result, we present the following lemmas, needed for the proof of Theorem 1:

Lemma 1. Under Assumptions 1-3, with the control law $u_i(t)$ defined in (6), the rotation angle $\hat{\alpha}_i(t)$ computed by each agent from (9) verifies $\hat{\alpha}_i(t) = \hat{\alpha}_0$, $\forall i \in \mathcal{N}$, $\forall t$. $\hat{\alpha}_0$ is a time-constant value equivalent to the rotation angle of the desired geometric spatial configuration, with respect to an arbitrary global reference frame, that minimizes the cost function (10) $\forall t$.

Proof 1. Define the term $T_i \equiv tan(\hat{\alpha}_i(t))$:

$$T_i = \frac{\sum_{k\in\mathcal{N}_i}\sum_{j\in\mathcal{N}_i}\hat{q}_{kj}^T(t)c_{kj}^{\perp}}{\sum_{k\in\mathcal{N}_i}\sum_{j\in\mathcal{N}_i}\hat{q}_{kj}^T(t)c_{kj}} \tag{13}$$

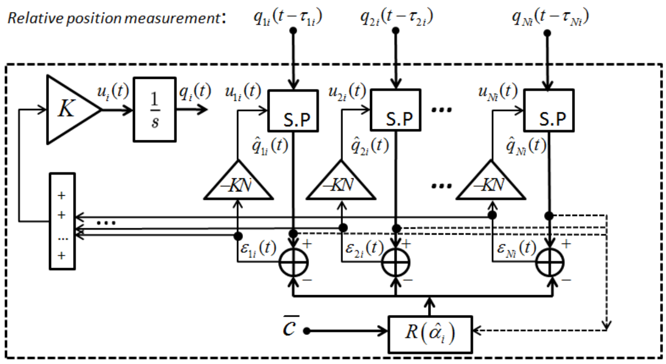

Fig. 1. Delay compensation control scheme for agent i: each Smith Predictor subsystem (labelled as S.P and detailed in Fig. 2) computes a delay-free prediction of each relative position $\hat{q}_{ki}(t)$ from the delayed measurement $q_{ki}(t-\tau_{ki})$ and $u_{ki}(t) = -KN\varepsilon_{ki}(t)$. The prediction $\hat{q}_{ki}(t)$ is used both to compute the rotation angle $\hat{\alpha}_i(t)$ and the control law $u_i(t)$ by means of (9) and (6), respectively. The parameter $\bar{c}$ has been introduced with the aim to simplify the scheme: it involves the references: $c_{1i}, \cdots, c_{N,i}$

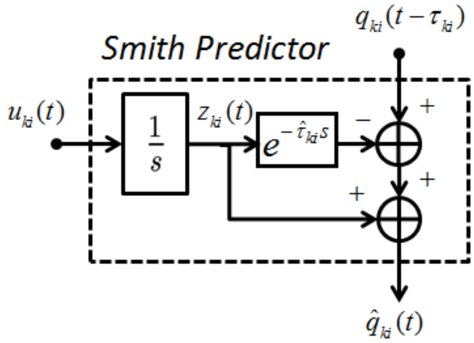

Fig. 2. Implementation details of each Smith Predictor (S.P.) subsystem from Fig. 1.

where $\hat{q}_{kj} = \hat{q}_{ki} - \hat{q}_{ji}$ (see (9) and (12)). Denoting $P_k^{\perp} = \sum_k\sum_j\hat{q}_{ki}^T(t)c_{kj}^{\perp}$, $P_k = \sum_k\sum_j\hat{q}_{ki}^T(t)c_{kj}$, $P_j^{\perp} = \sum_k\sum_j\hat{q}_{ji}^T(t)c_{kj}^{\perp}$, $P_j = \sum_k\sum_j\hat{q}_{ji}^T(t)c_{kj}$, the above expression yields:

$$T_i = \frac{P^{\perp}}{P} \tag{14}$$

where $P = P_k - P_j$ and $P^{\perp} = P_k^{\perp} - P_j^{\perp}$. The time derivative of T_i yields:

$$\frac{d}{dt}T_i(t) = \sum_{k\in\mathcal{N}_i}\sum_{i\in\mathcal{N}_i}\left(\frac{\partial}{\partial\hat{q}_{ki}}T_i(t)\right)^T\left(\frac{d}{dt}\hat{q}_{ki}(t)\right) + \tag{15}$$
$$+\sum_{k\in\mathcal{N}_i}\sum_{j\in\mathcal{N}_i}\left(\frac{\partial}{\partial\hat{q}_{ji}}T_i(t)\right)^T\left(\frac{d}{dt}\hat{q}_{ji}(t)\right)$$

where $\hat{q}_{kj}(t)$ is defined in (12). One the one hand, taking into account that:

$$\frac{\partial P}{\partial\hat{q}_{ki}} = c_{kj}, \qquad \frac{\partial P^{\perp}}{\partial\hat{q}_{ki}} = c_{kj}^{\perp} \tag{16}$$
$$\frac{\partial P}{\partial\hat{q}_{ji}} = -c_{kj}, \qquad \frac{\partial P^{\perp}}{\partial\hat{q}_{ji}} = -c_{kj}^{\perp}$$

we have:

$$\frac{\partial}{\partial \hat{q}_{ki}} T_i(t) = \frac{P c_{kj}^{\perp} - P^{\perp} c_{kj}}{P^2} \tag{17}$$
$$\frac{\partial}{\partial \hat{q}_{ji}} T_i(t) = \frac{-P c_{kj}^{\perp} + P^{\perp} c_{kj}}{P^2}$$

the transpose of the above terms yield respectively:

$$\left(\frac{\partial}{\partial \hat{q}_{ki}} T_i(t)\right)^T = \frac{P c_{kj}^{\perp T} - P^{\perp} c_{kj}^T}{P^2} \tag{18}$$
$$\left(\frac{\partial}{\partial \hat{q}_{ji}} T_i(t)\right)^T = \frac{-P c_{kj}^{\perp T} + P^{\perp} c_{kj}^T}{P^2}$$

On the other hand, from the definition of $\hat{q}_{ki}(t)$ in (12), we have:

$$\frac{d}{dt}\hat{q}_{ki}(t) = \frac{d}{dt} z_{ki} - \frac{d}{dt} z_{ki}(t-\hat{\tau}_{ki}) + \frac{d}{dt} q_{ki}(t-\tau_{ki}) \tag{19}$$
$$\frac{d}{dt}\hat{q}_{ji}(t) = \frac{d}{dt} z_{ji} - \frac{d}{dt} z_{ji}(t-\hat{\tau}_{ji}) + \frac{d}{dt} q_{ji}(t-\tau_{ji})$$

From the definition of $\dot{z}_{ki}$ in (11) we can write:

$$\frac{d}{dt} z_{ki}(t) = -KN\left(\hat{q}_{ki}(t) - R(\hat{\alpha}_i(t))c_{ki}\right) \tag{20}$$
$$\frac{d}{dt} z_{ki}(t-\hat{\tau}_{ki}) = -KN\left(\hat{q}_{ki}(t-\hat{\tau}_{ki}) - R(\hat{\alpha}_i(t-\hat{\tau}_{ki}))c_{ki}\right)$$

and

$$\frac{d}{dt} z_{ji}(t) = -KN\left(\hat{q}_{ji}(t) - R(\hat{\alpha}_i(t))c_{ji}\right) \tag{21}$$
$$\frac{d}{dt} z_{ji}(t-\hat{\tau}_{ji}) = -KN\left(\hat{q}_{ji}(t-\hat{\tau}_{ji}) - R(\hat{\alpha}_i(t-\hat{\tau}_{ji}))c_{ji}\right)$$

Also, from $u_i(t)$ in (6) we have:

$$\begin{aligned} \frac{d}{dt} q_{ki}(t-\tau_{ki}) &= \dot{q}_k(t-\tau_{ki}) - \dot{q}_i(t-\tau_{ki}) = \\ &= K\sum_m \left(\hat{q}_{mk}(t-\tau_{ki}) - R(\hat{\alpha}_k(t-\tau_{ki}))c_{mk}\right) - \\ &- K\sum_m \left(\hat{q}_{mi}(t-\tau_{ki}) - R(\hat{\alpha}_i(t-\tau_{ki}))c_{mi}\right) \end{aligned} \tag{22}$$

and

$$\begin{aligned} \frac{d}{dt} q_{ji}(t-\tau_{ji}) &= \dot{q}_j(t-\tau_{ji}) - \dot{q}_i(t-\tau_{ji}) = \\ &= K\sum_m \left(\hat{q}_{mj}(t-\tau_{ji}) - R(\hat{\alpha}_j(t-\tau_{ji}))c_{mj}\right) - \\ &- K\sum_m \left(\hat{q}_{mi}(t-\tau_{ji}) - R(\hat{\alpha}_i(t-\tau_{ji}))c_{mi}\right) \end{aligned} \tag{23}$$

Notice from (9) that $\hat{\alpha}_i(t)$ is a common expression for all the agents. Therefore, we have $\hat{\alpha}_k(t) = \hat{\alpha}_j(t) = \hat{\alpha}_i(t) \equiv \hat{\alpha}(t)$. Therefore, denoting $R(t) \equiv R(\hat{\alpha}(t))$ the expressions (22) and (23) can be respectively rearranged on the following form:

$$\frac{d}{dt} q_{ki}(t-\tau_{ki}) = -KN\left(\hat{q}_{ki}(t-\tau_{ki}) - R(t-\tau_{ki})c_{ki}\right) \tag{24}$$
$$\frac{d}{dt} q_{ji}(t-\tau_{ji}) = -KN\left(\hat{q}_{ji}(t-\tau_{ji}) - R(t-\tau_{ji})c_{ji}\right)$$

If we set $\hat{\tau}_{ki} = \tau_{ki}$ and $\hat{\tau}_{ji} = \tau_{ji}$, from (20), (21) and (24) we have that $\frac{d}{dt} q_{ki}(t-\hat{\tau}_{ki}) = \frac{d}{dt} z_{ki}(t-\hat{\tau}_{ki})$, $\frac{d}{dt} q_{ji}(t-\hat{\tau}_{ji}) = \frac{d}{dt} z_{ji}(t-\hat{\tau}_{ji})$ and therefore (19) yields:

$$\frac{d}{dt}\hat{q}_{ki}(t) = -KN\left(\hat{q}_{ki}(t) - R(t)c_{ki}\right) = -KN\varepsilon_{ki} \tag{25}$$
$$\frac{d}{dt}\hat{q}_{ji}(t) = -KN\left(\hat{q}_{ji}(t) - R(t)c_{ji}\right) = -KN\varepsilon_{ji}$$

where $\varepsilon_{ki}(t)$ is defined in (7). Replacing (18) and (25) into (15) we obtain:

$$\frac{d}{dt} T_i(t) = -KN\sum_k\sum_j \left(\frac{P c_{kj}^{\perp T} - P^{\perp} c_{kj}^T}{P^2}\right)\left(\varepsilon_{ki}(t) - \varepsilon_{ji}(t)\right) \tag{26}$$

Taking into account that $\hat{\alpha}_i(t)$ is the same for all the agents, we can see that $\varepsilon_{ki}(t) - \varepsilon_{ji}(t) = \varepsilon_{kj}(t) = \hat{q}_{kj}(t) - R(t)c_{kj}$. Then, the above expression writes:

$$\frac{d}{dt} T_i(t) = -KN\sum_k\sum_j \left(\frac{\left(P c_{kj}^{\perp T} - P^{\perp} c_{kj}^T\right)\left(\hat{q}_{kj}(t) - R(t)c_{kj}\right)}{P^2}\right) \tag{27}$$

Rearranging terms we obtain:

$$\begin{aligned} \frac{d}{dt} T_i(t) &= -KN\frac{P\sum_k\sum_j c_{kj}^{\perp T}\hat{q}_{kj}(t) - P^{\perp}\sum_k\sum_j c_{kj}^T \hat{q}_{kj}(t)}{P^2} + \\ &+ KN\sum_k\sum_j \left(\frac{P c_{kj}^{\perp T} R(t)c_{kj} - P^{\perp} c_{kj}^T R(t) c_{kj}}{P^2}\right) \end{aligned} \tag{28}$$

Noting the definitions of P and $P^{\perp}$, the above expression yields:

$$\begin{aligned} \frac{d}{dt} T_i(t) &= -KN\frac{PP^{\perp} - P^{\perp}P}{P^2} + \\ &+ KN\sum_k\sum_j \left(\frac{P c_{kj}^{\perp T} R(t)c_{kj} - P^{\perp} c_{kj}^T R(t) c_{kj}}{P^2}\right) \end{aligned} \tag{29}$$

and therefore, noting that $PP^{\perp} = P^{\perp}P$, (29) can be simplified as:

$$\frac{d}{dt} T_i(t) = KN\sum_k\sum_j \left(\frac{P c_{kj}^{\perp T} R(t)c_{kj} - P^{\perp} c_{kj}^T R(t) c_{kj}}{P^2}\right) \tag{30}$$

Given the fact that:

$$c_{kj}^T R(t) c_{kj} = cos(\hat{\alpha}_i)||c_{kj}||^2 \tag{31}$$
$$c_{kj}^{\perp T} R(t) c_{kj} = sin(\hat{\alpha}_i)||c_{kj}||^2$$

we can rewrite (30) as:

$$\frac{d}{dt} T_i(t) = KN\sum_k\sum_j ||c_{kj}||^2\left(Psin(\hat{\alpha}_i) - P^{\perp}cos(\hat{\alpha}_i)\right) \tag{32}$$

Taking into account from (14) that $P^{\perp} = P\ tan(\hat{\alpha}_i)$ we have $P^{\perp}cos(\hat{\alpha}_i) = Psin(\hat{\alpha}_i)$ and therefore $\frac{d}{dt}T_i(t) = 0$. Since $\hat{\alpha}_i$ cannot change its quadrant due to the properties of the controller (as argued in Aranda et al. (2015)), we have $\frac{d}{dt}\hat{\alpha}_i(t) = 0$. Finally, taking into account that the expression (9) is the same for all the agents and the fact that the available information of the relative positions at the initial instant $\bar{\tau}$ in which the agents start moving (see Assumption 1) is also the same for all of them, we conclude that $\hat{\alpha}_i(t) = \hat{\alpha}_0$. Evidently, $\hat{\alpha}_0$ is time-constant from the proved fact that $\frac{d}{dt}\hat{\alpha}_i(t) = 0$.

Lemma 2. The time derivative of the relative position between agents verifies $\dot{q}_{ki}(t) = -KN\varepsilon_{ki}(t)$, $\forall t \geq \bar{\tau}$, where $\varepsilon_{ki}(t)$ is defined in (7).

Proof 2. From Lemma 1 we have $\hat{\alpha}_i(t) \equiv \hat{\alpha}_0$. Denoting $R_0 = R(\hat{\alpha}_0)$, from the expressions (6) and (7), the term $\dot{q}_{ki}(t)$ yields:

$$\begin{aligned} \dot{q}_{ki}(t) &= \dot{q}_i(t) - \dot{q}_j(t) = u_i(t) - u_j(t) = \\ &= K\left(\sum_k \left(\hat{q}_{ki}(t) - \hat{q}_{kj}(t)\right) - R_0\sum_k\left(c_{ki} - c_{kj}\right)\right) = \\ &= -KN\left(\hat{\dot{q}}_{ki}(t) - R_0 c_{ki}\right) = -KN\varepsilon_{ki}(t) \end{aligned} \tag{33}$$

Lemma 3. Under Assumptions 1-3, the prediction of the relative position made by each agent with the proposed scheme, $\hat{q}_{ki}(t)$, just matches with the actual relative position $q_{ki}(t)$, i.e., $q_{ki}(t) - \hat{q}_{ki}(t) = 0$, $\forall t > \bar{\tau}$.

Proof 3. First, denote $d_{ki}(t) = q_{ki}(t) - \hat{q}_{ki}(t)$. On the one hand, from (12), we have:

$$d_{ki}(t) = q_{ki}(t) - z_{ki}(t) + z_{ki}(t-\tau_{ki}) - q_{ki}(t-\tau_{ki}) \tag{34}$$

From (11) and the initial condition $z_{ki}(0) = 0$ we have $z_{ki}(t) = 0$, $\forall t \leq \bar{\tau}$. On the other hand, from Assumption 1 it can be seen that $q_{ki}(t)$ is time-constant when $t \leq \bar{\tau}$. Therefore, it is easy to deduce from (34) that $d_{ki}(\bar{\tau}) = 0$. On the other hand, the time derivative of $d_{ki}(t)$ is:

$$\dot{d}_{ki}(t) = \dot{q}_{ki}(t) - \dot{z}_{ki}(t) + \dot{z}_{ki}(t-\tau_{ki}) - \dot{q}_{ki}(t-\tau_{ki}) \tag{35}$$

Taking into account that $\dot{z}_{ki}(t) = -KN\varepsilon_{ki}(t)$, from the definition of the S.P. scheme in (11), and the fact that $\dot{q}_{ki}(t) = -KN\varepsilon_{ki}(t), \forall t \geq \bar{\tau}$ (see Lemma 2), we can ensure that $\dot{d}_{ki}(t) = 0, \forall t \geq \bar{\tau}$

The proof of the asymptotic stability of the overall system is given below:

Theorem 1. Under Assumptions 1-3, the errors $\varepsilon_{ki}(t)$ are globally exponentially stable, regardless of the value of τ_{ki}:

Proof 4. From Lemma 1, we have that $\dot{R}(\hat{\alpha}_i(t))c_{ki} = 0$. The time derivative of $\varepsilon_{ki}(t)$ defined in (7) is therefore $\dot{\varepsilon}_{ki}(t) = \dot{\hat{q}}_{ki}(t)$. Since $\dot{d}_{ki}(t) = \dot{q}_{ki}(t) - \dot{\hat{q}}_{ki}(t) = 0, \forall t \geq \bar{\tau}$ (Lemma 2), we have that $\dot{\hat{q}}_{ki}(t) = \dot{q}_{ki}(t)$. Applying Lemma 3, we have $\dot{\hat{q}}_{ki}(t) = -KN\varepsilon_{ki}(t)$. Then, replacing into the above expression we obtain $\dot{\varepsilon}_{ki}(t) = -KN\varepsilon_{ki}(t)$. Therefore

$$\varepsilon_{ki}(t) = \begin{cases} \varepsilon_{ki}(\bar{\tau})e^{-KN(t-\bar{\tau})} & t \geq \bar{\tau} \\ 0 & t < \bar{\tau} \end{cases} \tag{36}$$

and then:

$$lim_{t\to\infty}\varepsilon_{ki}(t) = 0 \tag{37}$$

Lemma 4. The internal state $z_{ki}(t)$ from the Smith Predictor converges exponentially to the value $q_{ki}(0) - R(\hat{\alpha}_0)c_{ki}$, which shows clearly that the S.P. is internally stable.

Proof 5. Let us write:

$$z_{ki}(t) = z_{ki}(0) + \int_{s=0}^{t} \dot{z}_{ki}(s)ds \tag{38}$$

From the initial condition $z_{ki}(0) = 0$ and (11), we have:

$$z_{ki}(t) = \int_{s=0}^{\bar{\tau}} 0 \cdot ds - \int_{s=\bar{\tau}}^{t} KN\varepsilon_{ki}(s)ds \tag{39}$$

Recall from the proof of Theorem 1 that:

$$\varepsilon_{ki}(t) = \varepsilon_{ki}(\bar{\tau})e^{-KN(t-\bar{\tau})}, \forall t \geq \bar{\tau} \tag{40}$$

Therefore, from the definitions (7), (12), and the fact that $q_{ki}(t_1) = q_{ki}(t_2), \forall t_1, t_2 < \bar{\tau}$ because $u_i(t) = 0, \forall t < \bar{\tau}$, we finally have from (39) that:

$$z_{ki}(t) = \begin{cases} \varepsilon_{ki}(\bar{\tau})\left(e^{-KN(t-\bar{\tau})} - 1\right) & t \geq \bar{\tau} \\ 0 & t < \bar{\tau} \end{cases} \tag{41}$$

Thus, it can be straighforwardly deduced that $z_{ki}(t)$ converges exponentially to $lim_{t\to\infty}z_{ki}(t) = -\varepsilon_{ki}(\bar{\tau}) = R(\hat{\alpha}_0)c_{ki} - q_{ki}(0)$.

5. SIMULATION RESULTS

The effectiveness of the proposed delay compensation control scheme is illustrated through some simulation results in this section. In the examples, we consider 12 agents ($N = 12$), where the initial positions of each agent are set arbitrarely. The objective is to move all the agents to the desired geometric configuration depicted in Fig. 3. The control gain has been chosen $K = 10^{-3}$ to perform all the simulations.

The first simulation is made by setting arbitrarely the time delays as depicted in Table (5) (values in ms), where $\tau_{ki} \leq \bar{\tau} = 500ms$. Such delays have been intentionally chosen large enough to lead the overall system to instability with the control law (4). Nevertheless, by using the proposed control scheme (see Section 3), the overall system converges to the desired configuration, such as can be appreciated from the trajectories depicted in Fig. 4 (upper part). Also, the norm of the velocities and the rotation angle of the reference pattern $\hat{\alpha}_i$ are depicted in the lower part on Fig. 4 (left and right sides, respectively). Note that all the norm velocities converge exponentially to zero. Note also that the rotation angles computed by each agent from (9) are the same: $\hat{\alpha}_i = \hat{\alpha}_0 = -0.2591$. These facts reveal that the nominal performance is achieved due to the delay compensation control scheme. The next simulations take into account the existence of an estimation error $e_\tau = 15ms$ on the delays. In such a way, $\hat{\tau}_{ki} = \tau_{ki} - e_\tau$. The following three cases are considered: $\bar{\tau} = 100ms$, $\bar{\tau} = 200ms$ and $\bar{\tau} = 500ms$, where the same values for time delays in (5) scaled by $1/5$ and $2/5$ have been chosen for case 1 and 2, respectively. Fig. 5 shows the trajectories followed by the agents for all the simulations: when no delay compensation is implemented, it can be clearly appreciated in the left column on Fig. 5 from top (first case) to bottom (third case) how the system performance is degraded, leading to instability in the third case. This behavior can be also seen on the evolution of the rotation angle and the norm velocities (left column on Fig. 6 and 7). The right column on Fig. 5,6 and 7 depicts the system trajectories, rotation angle $\hat{\alpha}_i$ and norm velocities using the delay compensation method. Note that, even under some error on the delay estimation, the trajectories are hardly affected by such delay mismatches, leading to a significant performance enhancement compared to the case of no delay compensation. However, the presence of delay mismatches leads to some transient on the estimation of the rotation angle. It can be seen that the greater is the upper bound for delay $\bar{\tau}$, the larger is the settling time for the rotation angle. This fact points out that the negative impact of delay mismatches is greater when $\bar{\tau}$ grows, even when the delay mismatch keeps constant.

τ_{ki}	τ_{k1}	τ_{k2}	τ_{k3}	τ_{k4}	τ_{k5}	τ_{k6}	τ_{k7}	τ_{k8}	τ_{k9}	$\tau_{k,10}$	$\tau_{k,11}$	$\tau_{k,12}$
τ_{1i}	347	355	376	407	459	284	345	53	91	201	169	288
τ_{2i}	159	377	128	122	143	235	374	481	132	38	450	30
τ_{3i}	475	138	253	465	379	6	225	2	73	120	185	117
τ_{4i}	17	340	350	175	377	169	42	387	68	62	56	177
τ_{5i}	219	328	445	98	190	81	114	409	435	92	390	411
τ_{6i}	191	81	500	126	284	397	457	434	290	120	195	8
τ_{7i}	383	59	274	308	38	156	76	42	275	209	121	22
τ_{8i}	398	249	69	237	27	264	413	200	72	25	202	84
τ_{9i}	93	480	75	176	265	83	269	130	500	451	48	325
$\tau_{10,i}$	245	170	129	415	390	301	498	400	311	472	66	366
$\tau_{11,i}$	223	293	420	293	467	131	39	216	175	245	471	324
$\tau_{12,i}$	323	112	127	275	65	327	221	455	257	245	478	225

Table 1. Time delay values τ_{ki} used to perform the simulations.

Note also that, in all three cases, the order of magnitude of the perturbation on $\hat{\alpha}_i$ is not large enough to have a visible impact on the trajectories. The norm of the average error prediction on the relative position of each agent $d_i = \frac{1}{N}\sum_{k\in\mathcal{N}_i}||q_{ki} - \hat{q}_{ki}||$ is

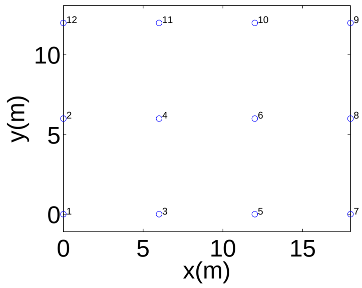

Fig. 3. Desired geometric configuration.

depicted in the left column on Fig. 8. It can be seen that the delay mismatches also lead to some transient, but the steady value for the average error $||d_i||$ is zero. The right column on Fig. 8 shows a comparison of the average cost function $J(t) = \frac{1}{N}\sum_{i=1}^{N} J_i(t)$, with J_i defined in (1), between the following three cases: (i) no delay compensation, (ii) delay compensation (S.P.) with delay mismatch ($e_\tau = 15ms$) and (iii) delay compensation with no delay mismatch ($e_\tau = 0ms$). From the top to the bottom, we have the three cases: $\bar{\tau} = 100ms$, $\bar{\tau} = 200ms$; and $\bar{\tau} = 500ms$ respectively. In the last case, it can be seen that $J(t)$ is unstable without delay compensation. Also, it can be appreciated that such delay mismatches does not affect significantly to the convergence of $J(t)$.

The last simulations (see Fig. 9) have been performed by setting $\bar{\tau} = 500ms$ (same time delay values in (5)), but considering bigger delay mismatches: $e_\tau = 75ms$, $e_\tau = 125ms$, and $e_\tau = 250ms$ respectively. It can be appreciated how the performance degrades as the delay mismatch grows. However, despite the evident degradation, the overall system keeps the stability when the delay mismatch even reaches 50% with respect to the actual delay. It's worthwile to recall that, without delay compensation, the system with the proposed delay values is unstable.

6. DISCUSSION AND CONCLUSION

In this paper we have presented a time delay compensation method based on the Smith Predictor applied to the stabilization of a group of mobile agents to a desired geometric configuration. From the given results, the idea of using S.P. to improve the overall performance seems promising. It has been also illustrated by simulation that, even in the case of relatively small error in the estimated delays, the proposed scheme improves with respect to the case of no delay compensation. We believe that an exhaustive analysis of robustness against delay mismatches is an interesting matter of future research. In this direction, our future work is aimed at providing an upper bound for the error on the delay estimation such that the stability of the overall system is guaranteed. Another appealing extension of this work of practical interest is the application of delay compensation methods to nonholonomic kinematic agents.

REFERENCES

Aranda, M., López-Nicolás, G., Sagüés, C., and Zavlanos, M.M. (2015). Coordinate-free formation stabilization based on relative position measurements. *Automatica*, 57, 11–20.

Coogan, S. and Arcak, M. (2012). Scaling the size of a formation using relative position feedback. *Automatica*, 48(10), 2677–2685.

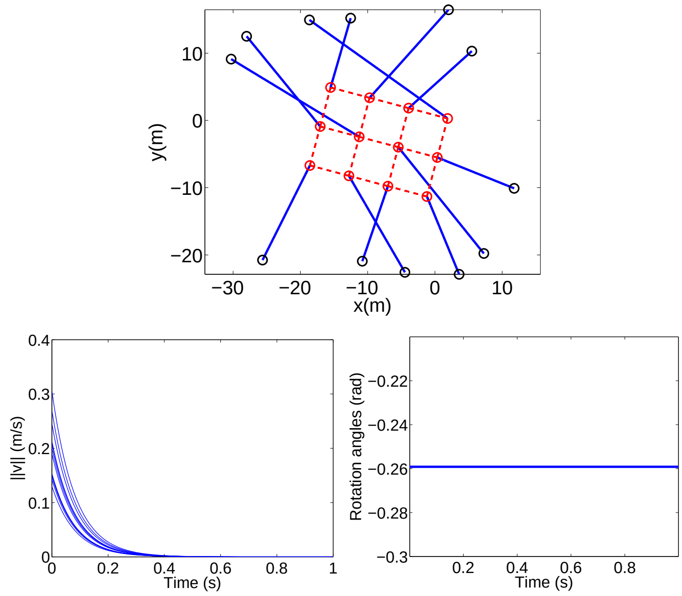

Fig. 4. Simulation results using the proposed control scheme with time delays $\tau_{ki} = \bar{\tau} = 500ms$ and no delay mismatches ($\hat{\tau}_{ki} = \tau_{ki}$). Upper figure: trajectories followed by each agent converging to the desired geometric configuration. Lower left-side: Norm velocities of each agent, Lower right-side: Estimation of the rotation angle $\hat{\alpha}_i = \hat{\alpha}_0 = -0.2591$, computed by each agent.

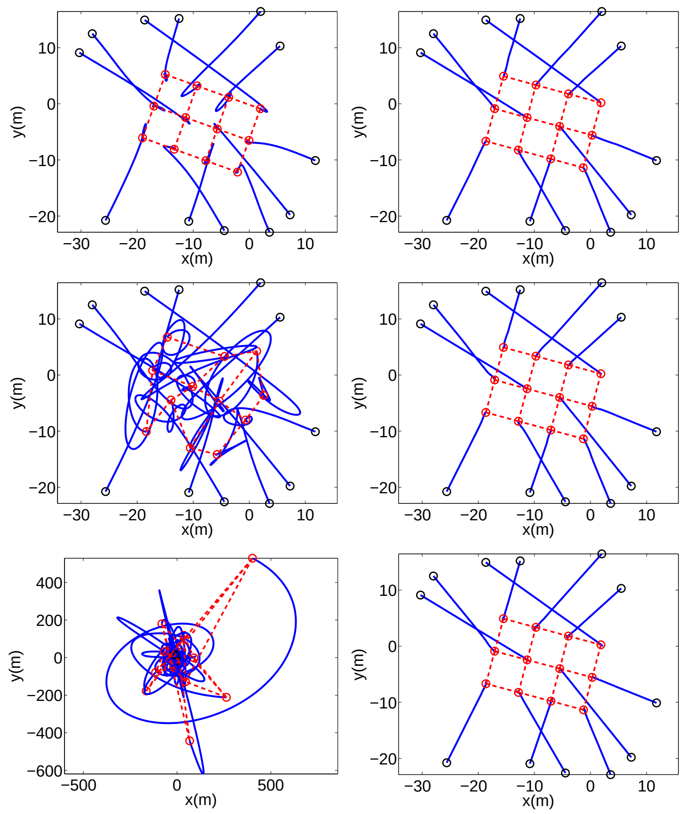

Fig. 5. Paths followed by each agent under time delays: left column, no delay compensation; right column, delay compensation with delay mismatch of $15ms$. Top: $\bar{\tau} = 100ms$, Middle: $\bar{\tau} = 200ms$, Bottom: $\bar{\tau} = 500ms$.

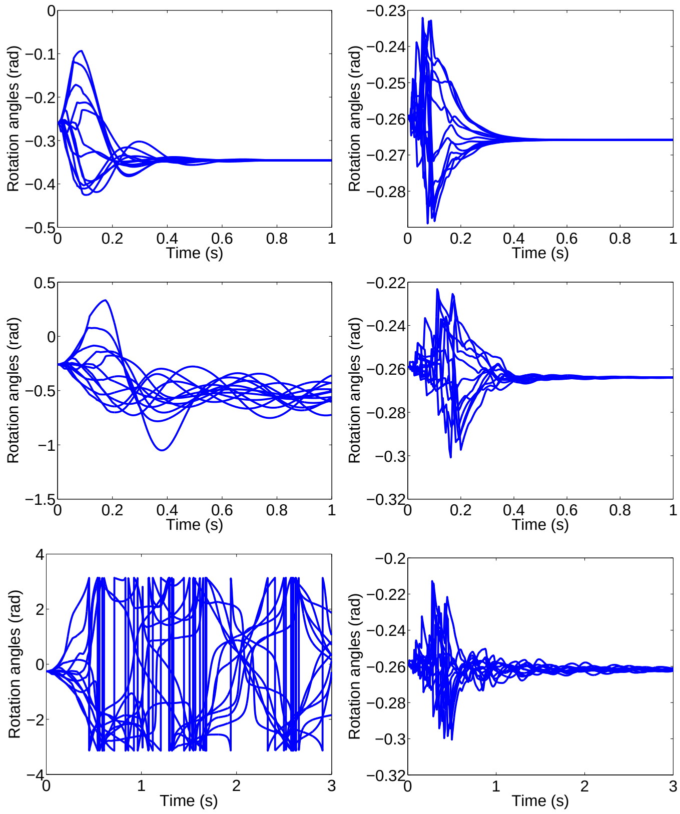

Fig. 6. Estimation of the rotation angle by each agent under time delays: left column, no delay compensation; right column, delay compensation with delay mismatch of $15ms$. Top: $\bar{\tau} = 100ms$, Middle: $\bar{\tau} = 200ms$, Bottom: $\bar{\tau} = 500ms$.

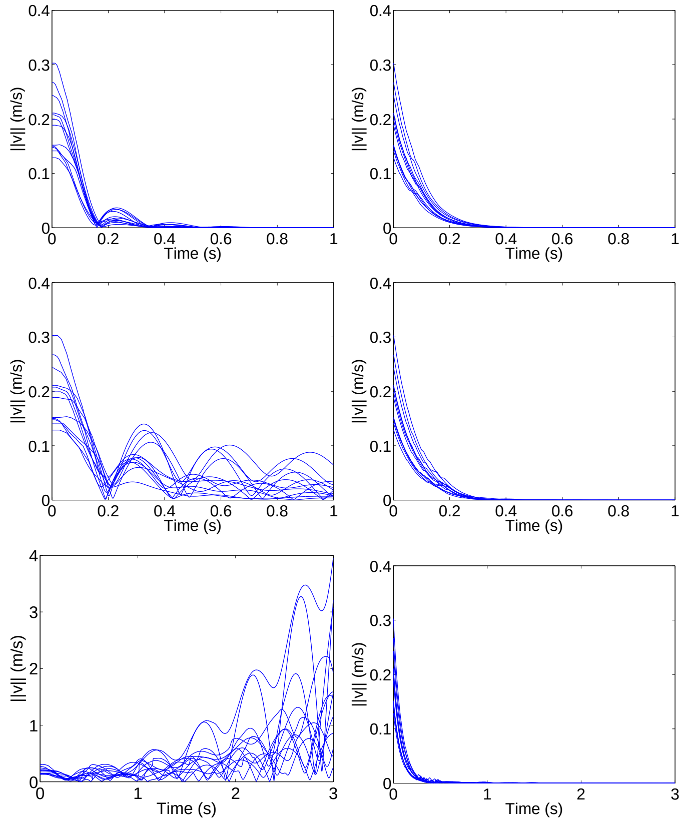

Fig. 7. Norm velocities corresponding to each agent under time delays: left column, no delay compensation; right column, delay compensation with delay mismatch of $15ms$. Top: $\bar{\tau} = 100ms$, Middle: $\bar{\tau} = 200ms$, Bottom: $\bar{\tau} = 500ms$.

Dimarogonas, D.V. and Kyriakopoulos, K.J. (2008). A connection between formation infeasibility and velocity alignment in kinematic multi-agent systems. *Automatica*, 44(10), 2648–2654.

Garrido, J., Vázquez, F., Morilla, F., and Normey-Rico, J.E. (2016). Smith predictor with inverted decoupling for square multivariable time delay systems. *International Journal of Systems Science*, 47(2), 374–388.

Gu, K., Chen, J., and Kharitonov, V.L. (2003). *Stability of time-delay systems*. Springer Science & Business Media.

Hang, C., Wang, Q.G., and Yang, X.P. (2003). A modified smith predictor for a process with an integrator and long dead time. *Industrial & engineering chemistry research*, 42(3), 484–489.

Khajorntraidet, C., Ito, K., and Shen, T. (2015). Adaptive time delay compensation for air-fuel ratio control of a port injection *SI* engine. In *54th Annual Conference of the Society of Instrument and Control Engineers of Japan (SICE), 2015*, 1341–1346.

Krick, L., Broucke, M.E., and Francis, B.A. (2009). Stabilisation of infinitesimally rigid formations of multi-robot networks. *International Journal of Control*, 82 (3), 423–439.

Mesbahi, M. and Egerstedt, M. (2010). *Graph theoretic methods in multiagent networks*. Princeton University Press.

Nedić, A. and Ozdaglar, A. (2010). Convergence rate for consensus with delays. *Journal of Global Optimization*, 47(3), 437–456.

Normey-Rico, J.E. (2007). *Control of dead-time processes*. Springer Science & Business Media.

Oh, K.K. and Ahn, H.S. (2014). Formation control and network localization via orientation alignment. *IEEE Transactions on Automatic Control*, 59(2), 540–545.

Oh, K.K., Park, M.C., and Ahn, H.S. (2015). A survey of multi-agent formation control. *Automatica*, 53, 424–440.

Papachristodoulou, A., Jadbabaie, A., and Münz, U. (2010). Effects of delay in multi-agent consensus and oscillator synchronization. *IEEE Transactions on Automatic Control*, 55(6), 1471–1477.

Ren, W. and Atkins, E. (2007). Distributed multi-vehicle coordinated control via local information exchange. *International Journal of Robust and Nonlinear Control*, 17(10-11), 1002–1033.

Roca, L., Guzman, J.L., Normey-Rico, J.E., and Berenguel, M. (2014). Filtered smith predictor with nonlinear model applied to a solar field. In *European Control Conference (ECC), 2014*, 773–777.

Sabattini, L., Secchi, C., and Fantuzzi, C. (2011). Arbitrarily shaped formations of mobile robots: artificial potential fields and coordinate transformation. *Autonomous Robots*, 30(4), 385–397.

Schwager, M., Julian, B.J., Angermann, M., and Rus, D. (2011). Eyes in the sky: Decentralized control for the deployment of robotic camera networks. *Proceedings of the IEEE*, 99(9), 1541–1561.

Smith, O. (1957). Closer control of loops with dead time. *Chemical Engineering Progress*, 53(5), 217–219.

Tian, Y.P. and Wang, Q. (2013). Global stabilization of rigid formations in the plane. *Automatica*, 49 (5), 1436–1441.

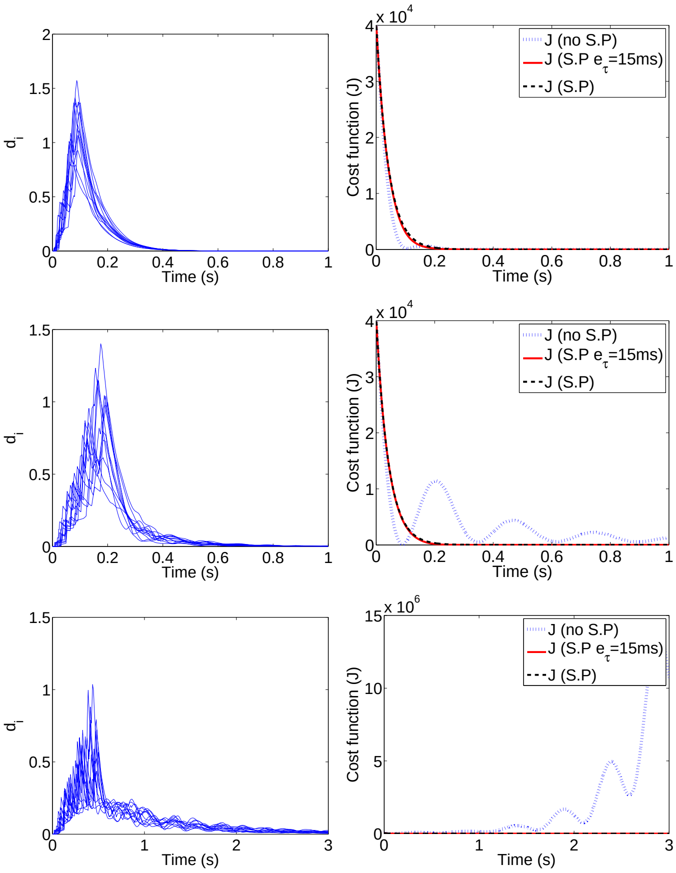

Fig. 8. Left column: Norm of the average error prediction on the relative position of each agent $d_i = \frac{1}{N}\sum_{k\in\mathcal{N}_i}||q_{ki} - \hat{q}_{ki}||$. Right column: Comparison of the cost function $J(t) = \frac{1}{N}\sum_{i=1}^{N} J_i(t)$ between the following three cases: (i) no delay compensation, (ii) delay compensation (S.P.) with delay mismatch ($e_\tau = 15ms$) and (iii) delay compensation with no delay mismatch ($e_\tau = 0ms$). First row: $\bar{\tau} = 100ms$; Second row: $\bar{\tau} = 200ms$; Third row: $\bar{\tau} = 500ms$.

Zavlanos, M.M. and Pappas, G.J. (2007). Distributed formation control with permutation symmetries. In *46th IEEE Conference on Decision and Control, 2007*, 2894–2899.

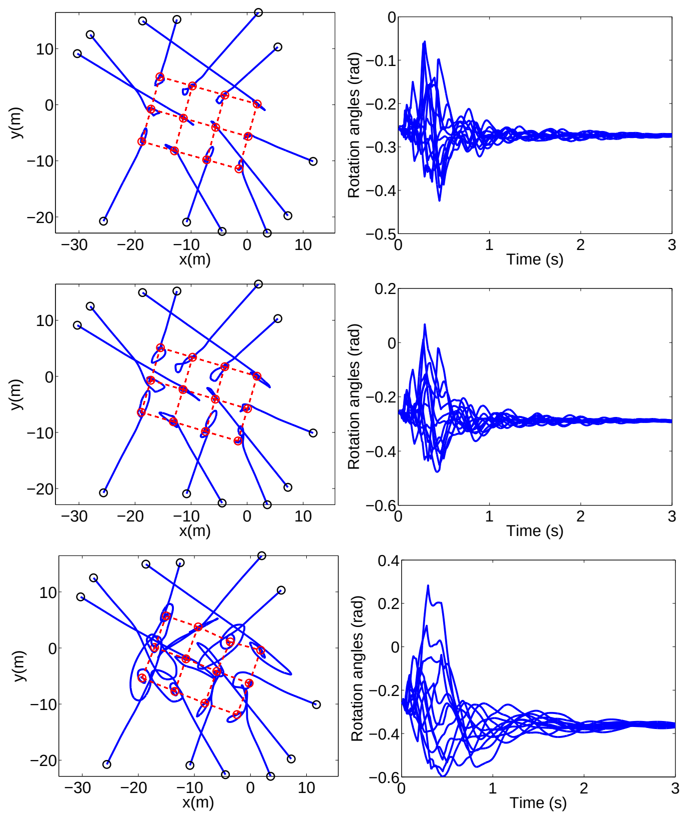

Fig. 9. Simulation results with upper bounde delay $\bar{\tau} = 500ms$ and bigger delay mismatches: left column, trajectories followed by each agent converging to the desired geometric configuration; right column, estimation of the rotation angle by each agent. Top: $e_\tau = 75ms$, Middle: $e_\tau = 125ms$, Bottom: $e_\tau = 250ms$.